LES-SPH model for weakly-compressible Navier-Stokes equations

M. Antuono, S. Marrone
CNR-INSEAN
Marine Technology Research Institute
Rome, Italy
matteo.antuono@cnr.it
salvatore.marrone@cnr.it

A. Di Mascio
CNR-IAC
Istituto per le applicazioni del calcolo
Rome, Italy
andrea.dimascio@cnr.it

A. Colagrossi
CNR-INSEAN and
Ecole Centrale Nantes,
LHEEA Res. Dept. (ECN and CNRS),
Nantes, France
andrea.colagrossi@cnr.it

***Abstract*—The Smoothed Particle Hydrodynamics (SPH) method is revisited within a Large Eddy Simulation (LES) perspective following the recent work of [1]. To this aim, LES filtering procedure is recast in a Lagrangian framework by defining a filter centred at the particle position that moves with the filtered fluid velocity. The Lagrangian formulation of LES is then used to re–interpret the SPH approximation of differential operators as a specific model based on the decomposition of the LES filter into a spatial and time filter.**

The derived equations represent a general LES-SPH scheme and contain terms that in part come from LES filtering and in part derive from SPH kernels. The last ones lead to additional terms (with respect to LES filtering) that contain fluctuations in space, requiring adequate modelling. Further, since the adopted LES filter differs from the classical Favre averaging for the density field, fluctuation terms also appear in the continuity equation.

In the paper, a closure model for all the terms is suggested and some simplifications with respect to the full LES-SPH model are proposed. The simplified LES model is formulated in a fashion similar to the diffusive SPH scheme of Molteni & Colagrossi [2] and the diffusive parameter is reinterpreted as a turbulent diffusive coefficient, namely ν_δ. In analogy with the turbulent kinetic viscosity ν_T, the diffusive coefficient is modelled through a Smagorinsky-like model and both ν_T and ν_δ are assumed to depend on the magnitude of the local strain rate tensor $\mathbb{D}$.

Some examples of the simplified model are reported for both 2D and 3D free-decaying homogeneous turbulence and comparisons with the full LES-SPH model are provided.

I. Introduction

Despite the increasing headways that, in recent years, have been made to push forward the SPH scheme, the solution of the Navier-Stokes equations through SPH still represents a challenging problem, mainly due to the lack of sound theoretical works about turbulence modelling in the Lagrangian context. In fact, the Direct Numerical Simulation (DNS) of high Reynolds number flows remains infeasible because of the wide range of scales to be resolved, that span from the macroscopic ones (determined by the length and velocity scales characterizing the problem at hand) to the smallest dissipation scales (determined by the physical properties of the fluid).

An alternative approach is the solution of the Navier-Stokes equations in the time- or ensemble-averaging formulation given by Reynolds averaged Navier–Stokes (RANS) equations, where all the space and time turbulent scales are modelled. As large eddy evolution strongly depends on the boundary conditions and on the size of the domain, universal modelling for RANS is extremely difficult. In SPH, several attempts to use RANS approaches exist, these all relying on a direct inclusion of $\kappa-\epsilon$ models (see, for example, [4], [5]).

The approach that lies in the middle between DNS and RANS is the Large Eddy Simulation (LES), where only sub–grid turbulent eddies are modelled by space filtering, whereas the largest eddies are directly simulated (see, for instance, the classical reviews by [8], [9]). LES modelling is expected to be easier than RANS modelling, because, when the discretization is fine enough, the small sub–grid eddies should be closer to an "isotropic and homogeneous" scenario and therefore much less dependent on the specific problem under investigation. This (and the increased computer power) is probably the reason that determined the success of LES approaches in the last years, possibly in conjunction with zonal approaches, like Detached Eddy Simulation (see the review in [11]), that bypass the strict requirements for boundary layer simulations. In addition to these considerations, there is a further crucial aspect that makes the LES approach most suited for modelling the Navier-Stokes equations in the SPH framework, i.e. the common use of a filtering procedure to represent the spatial differential operators.

At present, various works deal with the LES modelling in particle methods such as SPH, see for example [12], [13], [15]. In [1] a rigorous reformulation of LES filtering in a Lagrangian context is provided and, through a decomposition of the filter in its spatial and temporal components, a consistent LES-SPH model is derived. Such a model maintains the simple structure of the Lagrangian Navier–Stokes equations and contains additional terms (deriving from both the LES and SPH filtering procedures) that must be properly modelled.

In the present work we show that part of such additional terms play a secondary role in the flow dynamics and can be dropped. This allows us to derive a simplified version of the model described in [1] which proves to be much more manageable for practical applications. Remarkably, we find

that the simplified LES-SPH can formulated in a fashion similar to the diffusive scheme of Molteni & Colagrossi [2]. In this case, the coefficient of the term in the continuity equation has to be regarded as a turbulent diffusive term, hereinafter denoted δ_T and, along with the turbulent kinetic viscosity ν_T, it is represented through a Smagorinsky-like model In particular, this means that both ν_T and δ_T are assumed to depend on the magnitude of the local strain rate tensor $\mathbb{D}$.

II. Lagrangian Large Eddy Simulation

In the present section, we briefly recall the procedure to rewrite the Large Eddy Simulation in a Lagrangian fashion. The resulting scheme is used in the sequel to define a general LES-SPH modelling. In Lagrangian formalism, the Navier-Stokes equations for a barotropic weakly-compressible Newtonian fluid read:

$$\begin{cases} \dfrac{d\rho}{dt} = -\rho\,\nabla\cdot\boldsymbol{u}\,, \\ \dfrac{d\boldsymbol{u}}{dt} = -\dfrac{\nabla p}{\rho} + \nu\Delta\boldsymbol{u} + (\lambda'+\nu)\,\nabla\,(\nabla\cdot\boldsymbol{u})\,, \\ \dfrac{d\boldsymbol{x}}{dt} = \boldsymbol{u}\,, \qquad p = F(\rho)\,, \end{cases} \tag{1}$$

where $\boldsymbol{u}$ is the flow velocity, p and ρ denote the pressure and density fields respectively and F represents the state equation. The hypothesis that the fluid is weakly-compressible corresponds to assume:

$$\frac{dp}{d\rho} = c^2 \gg \max\left(\|\boldsymbol{u}\|^2\,, \frac{\delta p}{\rho}\right), \tag{2}$$

where $c = c(\rho)$ is the sound speed and δp denotes the maximum pressure variation. The viscosity coefficients ν, λ' indicate the ratios between the Lamé constants μ, λ and the density ρ. The fluid being weakly-compressible, ν and λ' are assumed constant. Now, let us define a Lagrangian filter with compact support in $\mathbb{R}^3\times\mathbb{R}$ as follows:

$$\phi = \phi\,(\,\tilde{\boldsymbol{x}}_p(t) - \boldsymbol{y}, t-\tau\,)\,. \tag{3}$$

The filter is supposed to depend only on $\|\tilde{\boldsymbol{x}}_p(t)-\boldsymbol{y}\|$ and $|t-\tau|$, and to be an even function with respect to both arguments. Here $\tilde{\boldsymbol{x}}_p(t)$ indicates the position of a material point that moves with the velocity

$$\boxed{\tilde{\boldsymbol{u}}(\tilde{\boldsymbol{x}}_p(t),t) = \int_{\mathbb{R}^3}\int_{\mathbb{R}} \phi(\tilde{\boldsymbol{x}}_p(t)-\boldsymbol{y}, t-\tau)\,\boldsymbol{u}(\boldsymbol{y},\tau)\,d\tau\,dV_y\,,} \tag{4}$$

that is:

$$\tilde{\boldsymbol{x}}_p(t) = \int_{t_0}^{t} \tilde{\boldsymbol{u}}(\,\tilde{\boldsymbol{x}}_p(\tau),\tau\,)\,d\tau\,. \tag{5}$$

Hereinafter, we refer to $\tilde{\boldsymbol{x}}_p$ and $\tilde{\boldsymbol{u}}$ as the filtered position and velocity, respectively. We underline that, unless the turbulent process may be regarded as an ergodic one, the time and space filtering procedures are not equivalent and do not correspond to an ensemble averaging. The use of a space-time filter is the most general formulation for Lagrangian problems and is specifically suited for particle methods.

Since the state equation is generally nonlinear, $\widetilde{F(\rho)}$ is different from $F\,(\tilde{\rho})$ and, consequently, the filtering procedure cannot be applied to both pressure and density. To avoid inconsistency, when we refer to *filtered* pressure we mean

$$\boxed{\tilde{p} = F\,(\tilde{\rho})\,.} \tag{6}$$

Under this hypothesis, we apply the filter in (3) to the Navier-Stokes equations for weakly-compressible flows and, integrating over $\mathbb{R}^3\times\mathbb{R}$, we obtain (see [1] for details):

$$\begin{cases} \dfrac{d\tilde{\rho}}{dt} = -\,\tilde{\rho}\,\nabla\cdot\tilde{\boldsymbol{u}} + \nabla\cdot\left[\,\tilde{\rho}\tilde{\boldsymbol{u}} - \widetilde{\rho\boldsymbol{u}}\,\right], \\ \dfrac{d\tilde{\boldsymbol{u}}}{dt} = -\dfrac{\nabla\tilde{p}}{\tilde{\rho}} + \nu\Delta\tilde{\boldsymbol{u}} + (\lambda'+\nu)\,\nabla\,(\nabla\cdot\tilde{\boldsymbol{u}}) \\ \qquad\qquad -\nabla\left[\,\widetilde{G(\rho)} - G(\tilde{\rho})\,\right] + \nabla\cdot\mathrm{T}_\ell + \widetilde{\boldsymbol{u}\,\nabla\cdot\boldsymbol{u}}\,, \\ \dfrac{d\tilde{\boldsymbol{x}}_p}{dt} = \tilde{\boldsymbol{u}}\,, \quad \tilde{p} = F\,(\tilde{\rho})\,, \quad G(\rho) = \displaystyle\int^{\rho}\frac{1}{s}\,\frac{dF}{ds}\,ds\,, \end{cases} \tag{7}$$

where

$$\boxed{\mathrm{T}_\ell = \tilde{\boldsymbol{u}}\otimes\tilde{\boldsymbol{u}} - \widetilde{\boldsymbol{u}\otimes\boldsymbol{u}}\,,}$$

the tensor T_ℓ being the Lagrangian equivalent of the sub-grid stress tensor. Note that the symbol d/dt now stands for the Lagrangian derivative following the filtered velocity field $\tilde{\boldsymbol{u}}$. It is to be noticed that the choice of the space–time filter (3) yields a system of equations that retains the simple Lagrangian structure of the unfiltered Navier–Stokes equations (i.e. a system of equations where the time derivative is computed on fluid particles that move with the filtered velocity). The same structure can be obtained by using a simple space filter, even though a different closure is required for the additional terms as a consequence of the absence of the time filter.

Finally, we observe that the space-time filter in the Lagrangian context is formally identical to the analogous operation in the Eulerian context. Consequently, it can be verified that the formal relations between filtered quantities with different kernel supports (e.g. Germano's identity [18]) still hold true and can possibly be applied for the development of dynamic models.

III. SPH approximation with a LES perspective

Using the results of the previous section, we are now in a position to define the main ingredients of a generic weakly-compressible LES-SPH model. First, we briefly recall the structure of SPH and, then, we proceed to the construction of the filtered LES-SPH equations.

The smoothing procedure used in all SPH approaches somehow recalls the one used to obtain the Lagrangian LES. The main differences between these filtering procedures is that SPH approaches adopt a filter ("kernel" in the SPH terminology) that depends only on the spatial variables ($\tilde{\boldsymbol{x}}_p -$

$\boldsymbol{y}$); furthermore, the smoothing procedure is not applied to the Navier-Stokes equations, but rather to the differential operators, that are replaced by their smoothed counterpart (see [19], [20]).

It is possible, nevertheless, to reinterpret the Lagrangian LES through the SPH approach. To this purpose, we split the filter ϕ into

$$\phi\,(\,\tilde{\boldsymbol{x}}_p(t)-\boldsymbol{y},t-\tau\,)\;=\;W(\,\tilde{\boldsymbol{x}}_p(t)-\boldsymbol{y}\,)\;\theta(\,t-\tau\,)\;, \qquad (8)$$

where W indicates the SPH kernel. In SPH notation, the smoothing procedure of a generic scalar field f is indicated as

$$\langle f\rangle\,(\,\tilde{\boldsymbol{x}}_p(t),t\,)\;=\;\int_{\mathbb{R}^3} W\,(\,\tilde{\boldsymbol{x}}_p(t)-\boldsymbol{y}\,)\;f(\boldsymbol{y},t)\,dV_y\,. \qquad (9)$$

Here, a time filtering alone is introduced by the symbol

$$\overline{f}\,(\boldsymbol{y},t)\;=\;\int_{\mathbb{R}}\theta\,(\,t-\tau\,)\;f(\boldsymbol{y},\tau)\,d\tau\,. \qquad (10)$$

From the above definitions

$$\tilde{f}\;=\;\langle\,\overline{f}\,\rangle\,. \qquad (11)$$

Note that, since $\tilde{\boldsymbol{x}}_p$ depends on time, time filtering and SPH smoothing (space filter) do not commute, i.e. $\langle\,\overline{f}\,\rangle\neq\overline{\langle f\rangle}$ (see [1] for more details). Since the time filter is the inner one, the overall LES-SPH scheme may be regarded as a spatial Lagrangian filter applied to a set of time-averaged variables. In this sense, the time filter may be thought as an implicit filter whose presence is accounted for through the modeling of the additional terms.

Now, suppose that we want to compute a high Reynolds number flow, for which LES filtering is required. Then, we need the filtered variables $\tilde{\boldsymbol{u}},\tilde{p},\tilde{\rho}$ for each fluid particle at positions $\tilde{\boldsymbol{x}}_p$; at the same time, we want to approximate the operators in equation (7) in the SPH fashion. Using equation (11), we write:

$$\nabla\cdot\tilde{\boldsymbol{u}}=\nabla\cdot\langle\overline{\boldsymbol{u}}\rangle=\langle\nabla\cdot\overline{\boldsymbol{u}}\rangle\,. \qquad (12)$$

Of course, we cannot use time–filtered quantities like $\overline{\boldsymbol{u}}$ to approximate the operator, because we can compute only space-time filtered variables $\tilde{\boldsymbol{u}},\tilde{\rho},\tilde{p}$ associated to the particles at position $\tilde{\boldsymbol{x}}_p$ that move with speed $\tilde{\boldsymbol{u}}$. However, note that, far from the boundaries, differentiation and space filtering commute and the operator is linear; therefore, the divergence of the filtered velocity can be recast as

$$\nabla\cdot\tilde{\boldsymbol{u}}=\langle\nabla\cdot\overline{\boldsymbol{u}}\rangle=\langle\nabla\cdot(\overline{\boldsymbol{u}}+\tilde{\boldsymbol{u}}-\tilde{\boldsymbol{u}})\rangle=\langle\nabla\cdot\tilde{\boldsymbol{u}}\rangle+\langle\nabla\cdot(\overline{\boldsymbol{u}}-\tilde{\boldsymbol{u}})\rangle\,.$$

For confined flows, the non-commutability of filtering and differentiation must be taken into account for a rigorous extension of the filtering close to the boundaries (i.e. in those points whose distance from the boundaries is smaller than the kernel radius). The above procedure can be applied to all the remaining operators. In particular, denoting by $\boldsymbol{u}',p'$ the small-scale "fluctuations" in space, namely:

$$\boldsymbol{u}'\;=\;\tilde{\boldsymbol{u}}\;-\;\overline{\boldsymbol{u}}\,,\qquad \boldsymbol{u}'\;=\;\tilde{p}\;-\;\overline{p}\,, \qquad (13)$$

the system (7) can be recast in SPH formalism as follows:

$$\begin{cases}\dfrac{d\tilde{\rho}}{dt}\;=\;-\,\tilde{\rho}\,\langle\nabla\cdot\tilde{\boldsymbol{u}}\rangle\;+\;\mathcal{C}_1\;+\;\mathcal{C}_2\,,\\[2ex]\dfrac{d\tilde{\boldsymbol{u}}}{dt}=-\dfrac{\langle\nabla\tilde{p}\rangle}{\tilde{\rho}}+\nu\langle\Delta\tilde{\boldsymbol{u}}\rangle+(\lambda'{+}\nu)\langle\nabla(\nabla\cdot\tilde{\boldsymbol{u}})\rangle+\mathcal{M}_1+\mathcal{M}_2\,,\\[2ex]\dfrac{d\tilde{\boldsymbol{x}}_p}{dt}\;=\;\tilde{\boldsymbol{u}}\,,\qquad\tilde{p}\;=\;F\,(\tilde{\rho})\;,\end{cases} \qquad (14)$$

where:

$$\mathcal{C}_1\;=\;\tilde{\rho}\,\langle\nabla\cdot\boldsymbol{u}'\rangle\,,\qquad\mathcal{C}_2\;=\;\nabla\cdot[\,\tilde{\rho}\,\tilde{\boldsymbol{u}}-\widetilde{\rho\,\boldsymbol{u}}\,]\,, \qquad (15)$$

$$\mathcal{M}_1\;=\;\frac{\langle\,\nabla p'\,\rangle}{\tilde{\rho}}-\nu\,\langle\,\Delta\boldsymbol{u}'\,\rangle-(\lambda'{+}\nu)\,\langle\,\nabla(\nabla\cdot\boldsymbol{u}')\,\rangle\,, \qquad (16)$$

$$\mathcal{M}_2\;=\;-\,\nabla\left[\,\widetilde{G(\rho)}-G(\tilde{\rho})\,\right]\;+\;\widetilde{\boldsymbol{u}\,\nabla\cdot\boldsymbol{u}}\;+\;\nabla\cdot\mathrm{T}_\ell\,. \qquad (17)$$

Here $\mathcal{C}_1$ and $\mathcal{M}_1$ come from the SPH approximation procedure and require a SPH closure, whereas $\mathcal{C}_2$ and $\mathcal{M}_2$ include all terms from the Lagrangian LES and require a LES closure. Incidentally, we note that the term $\mathcal{C}_2$ is not present in LES models for compressible flows where Favre-filtered variables are adopted (see, for example, [21]). The system (14) can be regarded as a general LES-SPH model. The specific closures adopted for terms $\mathcal{C}_1,\mathcal{C}_2,\mathcal{M}_1$ and $\mathcal{M}_2$ will define a whole family of methods based on a consistent inclusion of the LES approach in the SPH framework.

As anticipated in the Introduction, $\mathcal{C}_1,\mathcal{C}_2,\mathcal{M}_1$ and $\mathcal{M}_2$ can be simplified by dropping those contributions that are, in fact, negligible in the flow dynamics. In particular, as proved in [1], the terms depending on the small scale "fluctuations" $\boldsymbol{u}',p'$ play a secondary role and, therefore, $\mathcal{C}_1$ and $\mathcal{M}_1$ are dropped in the simplified LES-SPH model. Moreover, the weakly-compressibility assumption allows us to disregard those terms inside $\mathcal{M}_2$ that derive from the density and pressure variations (incidentally, when using a linear equation of state the term $\widetilde{G(\rho)}-G(\tilde{\rho})$ is identically null). This leads to the following simplified form:

$$\mathcal{M}_2\;\simeq\;\nabla\cdot\mathrm{T}_\ell\,. \qquad (18)$$

For what concerns the closures formulae for $\mathcal{C}_2$ and $\mathcal{M}_2$, we adopt a typical LES modelling. In particular, following [22] we write:

$$\mathcal{M}_2\;=\;\nabla\cdot\left[-\frac{q^2}{3}\,1\;-\;\frac{2}{3}\,\nu_T\,\mathrm{Tr}(\widetilde{\mathrm{D}})\,1\;+\;2\,\nu_T\,\widetilde{\mathrm{D}}\right]\,, \qquad (19)$$

where q^2 represents the turbulent kinetic energy, ν_T is the turbulent kinetic viscosity and $\widetilde{\mathrm{D}}$ is the strain-rate tensor, that is $\widetilde{\mathrm{D}}=(\nabla\tilde{\boldsymbol{u}}+\nabla\tilde{\boldsymbol{u}}^T)/2$. Similarly to [22], we assume:

$$q^2\;=\;2\,C_Y\,h^2\,\|\,\widetilde{\mathrm{D}}\,\|^2\,,\qquad\nu_T\;=\;(C_S\,h)^2\;\|\,\widetilde{\mathrm{D}}\,\|\,, \qquad (20)$$

where $\|\widetilde{\mathrm{D}}\|$ is a rescaled Frobenius norm, namely:

$$\|\,\widetilde{\mathrm{D}}\,\|\;=\;\sqrt{2\,\widetilde{\mathrm{D}}\!:\!\widetilde{\mathrm{D}}}\,, \qquad (21)$$

and h is kernel the smoothing length which is chosen as length scale of the LES filter. The dimensionless parameters C_Y and C_S are respectively called the Yoshizawa and Smagorinsky constants. In [22] $C_Y = 0.044$ is used while, regarding the Smagorinsky constant, $C_S = 0.12$ has been adopted like in [14] and in [15]. For a general discussion on the influence of compressibility in turbulent flows see e.g. [23]. Further, as commented in [25], also the first two terms in equation (19) are not relevant for the same reasons and, therefore, they are removed from the model.

For what concerns the term $\mathcal{C}_2$, we follow a similar approach and assume a Fick-like diffusion law. Specifically, we put:

$$\mathcal{C}_2 \;=\; \nabla \cdot [\, \tilde{\rho}\tilde{\boldsymbol{u}} - \widetilde{\rho \boldsymbol{u}} \,] \;=\; \nabla \cdot (\, \nu_\delta \, \nabla \tilde{\rho}) \;, \tag{22}$$

where ν_δ has the dimension of a kinetic viscosity and represents a turbulent diffusion coefficient. Similarly to the expression of ν_T, we assume the following structure:

$$\nu_\delta \;=\; (C_\delta \, h)^2 \; \| \, \widetilde{\mathrm{D}} \, \| \,, \tag{23}$$

where C_δ is a dimensionless coefficient. This has been set equal to 1.5 after some preliminary numerical experiments. A complete calibration is postponed to future works.

IV. The LES-SPH model

Both formulae in (19) and (22) have been modelled by using the standard SPH differential operators. In particular, we use the following expressions:

$$\mathcal{C}_2^{(i)} = \sum_j \nu_{ij}^\delta \, \boldsymbol{\mathcal{D}}_{ij} \cdot \nabla_i W_{ij} V_j \,, \quad \mathcal{M}_2^{(i)} = \sum_j \nu_{ij}^T \; \tilde{\pi}_{ij} \, \nabla_i W_{ij} V_j \,.$$

where

$$\boldsymbol{\mathcal{D}}_{ij} = \frac{2\,(\rho_i - \rho_j)\;\boldsymbol{x}_{ji}}{\|\boldsymbol{x}_{ji}\|^2}, \quad \nu_{ij}^\delta = \frac{2\,\nu_\delta^{(i)} \nu_\delta^{(j)}}{\nu_\delta^{(i)} + \nu_\delta^{(j)}}, \quad \nu_{ij}^T = \frac{2\,\nu_T^{(i)} \nu_T^{(j)}}{\nu_T^{(i)} + \nu_T^{(j)}}.$$

These derive from a straightforward generalization of the Laplacian of [26] and of the viscous term of [27]. Here $\tilde{\pi}_{ij}$ is the Monaghan and Gingold [28] viscosity term evaluated by using $\tilde{\boldsymbol{u}}_i$. The expressions for $\nu_T^{(i)}$ and $\nu_\delta^{(i)}$ are given in equations (20) and (23) while the strain-rate tensor is computed through the formula below (see [20]):

$$\widetilde{\mathrm{D}}_i = \frac{1}{2} \sum_j [(\tilde{\boldsymbol{u}}_j - \tilde{\boldsymbol{u}}_i) \otimes (\mathrm{L}_i \cdot \nabla W_{ij}) + (\mathrm{L}_i \cdot \nabla W_{ij}) \otimes (\tilde{\boldsymbol{u}}_j - \tilde{\boldsymbol{u}}_i)] V_j$$

where L_i indicates the gradient renormalization tensor (for details see [30]). The final LES-SPH scheme reads:

$$\begin{cases} \dfrac{d\rho_i}{dt} \;= -\rho_i \sum_j (\boldsymbol{u}_j - \boldsymbol{u}_i) \cdot \nabla_i W_{ij} V_j \\ \qquad\qquad + \sum_j \nu_{ij}^\delta \, \boldsymbol{\mathcal{D}}_{ij} \cdot \nabla_i W_{ij} V_j, \\ \dfrac{d\boldsymbol{u}_i}{dt} = \boldsymbol{g}_i - \dfrac{1}{\rho_i} \sum_j (p_i + p_j) \, \nabla_i W_{ij} V_j \\ \qquad\qquad + \sum_j \left(\nu + \nu_{ij}^T\right) \, \pi_{ij} \, \nabla_i W_{ij} V_j, \\ \dfrac{d\boldsymbol{r}_i}{dt} \;= \boldsymbol{u}_i, \qquad\qquad p_i = c_0^2 \, (\rho_i - \rho_0) \end{cases} \tag{24}$$

where the filtered variables are expressed in the usual form without the symbol $\widetilde{(\cdot)}$ in order to simplify the notation. Incidentally, we observe that the above system can be recast in the δ-SPH fashion (see [31], [32]) by using:

$$\boldsymbol{\mathcal{D}}_{ij} \;= 2 \left[(\rho_i - \rho_j) - \frac{1}{2} \, \left(\langle \nabla \rho \rangle_j^L + \langle \nabla \rho \rangle_i^L \right) \cdot \boldsymbol{x}_{ji} \right] \frac{\boldsymbol{x}_{ji}}{\|\boldsymbol{x}_{ji}\|^2}$$

The second term in parenthesis is introduced for stabilising the computations in presence of a free-surface (see [32]). Some preliminary test cases have been run with this term showing promising results. In any case, further studies will be addressed in future works.

The C2 Wendland kernel has been chosen for the spatial filter W and a fourth-order Runge-Kutta scheme has been implemented to advance in time the model. Furthermore, for the 2D simulations the packing algorithm described in [34] has been used to obtain the so-called "glass-configurations" for the initial particle positions. These configurations are preferable to the Cartesian lattice since they avoid the particle resettlement during the early stages of the evolution (see [35]).

A ratio $h/\Delta x = 2$ is used in all the simulations, this corresponding to about 50 particles (in 2D) in the kernel support. In order to evaluate the energy spectrum during the post-processing stage, the magnitude of the velocity fields have been interpolated on a uniform Cartesian mesh with spacing equal to Δx. For the interpolation of the SPH scattered data, a Moving Least Square technique has been used as described in [36].

V. Numerical results

A. Freely-decaying turbulence in 2D

The LES-SPH scheme described above has been firstly tested through simulations of free decay of two dimensional homogeneous turbulence, with different values of the viscosity and various discretizations.

The initial conditions were chosen similarly to those of the physical experiment described in [37] for a regular configuration with 64 vortices. These were cast in an array of 8×8 Taylor–Green vortices in a bi-periodic domain with size $L \times L$ (the reference length L is set equal to 1). The maximum value of the velocity field in the initial configuration is $U = 1$ while a positive constant value, namely $P_0 = 2\,\rho_0\,U^2$, has been added to the pressure field to avoid the onset of the so-called "tensile instability". The initial vorticity and pressure are shown in figure 1. In order to assess the influence of the LES-SPH model the simulations are performed also through the standard SPH scheme using only the Monaghan and Gingold approximation of the viscous stresses [28].

The simulations have been performed at $Re_l = lU/\nu = 125,000$, with $l = L/8$ the vortex size. For this case, three different particle discretizations were adopted, namely $l/h = 9, 18, 75$. These resolutions are all insufficient for a correct direct simulation using the standard SPH scheme but are fine enough for the proposed LES-SPH model. Indeed, it is possible to evaluate the discretization on the base of

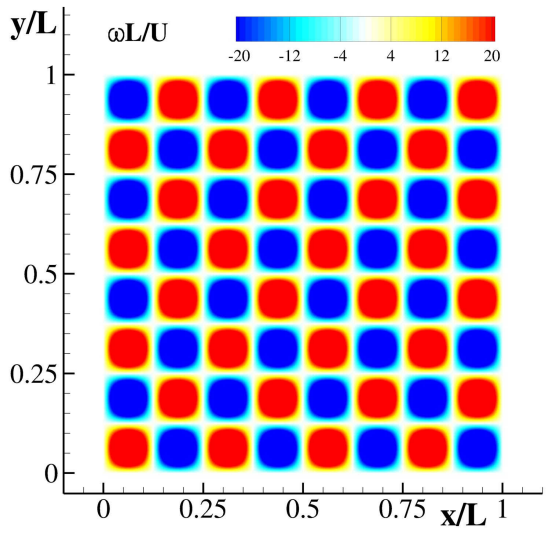

Fig. 1: Two-dimensional freely-decaying turbulence. Initial configuration: vorticity

the Reynolds cell number $Re_h = hU/\nu = \mathcal{O}(1)$. This means that the needed particle resolution should be at least $l/h = \mathcal{O}(10^5)$ for a fully resolved DNS. This is confirmed by the energy spectra of figure 2, where the solutions at the three different discretizations are reported for both the standard SPH scheme and the proposed LES-SPH model. For the two coarser particle resolutions, the energy distribution in frequency of the standard SPH is completely unrealistic, the

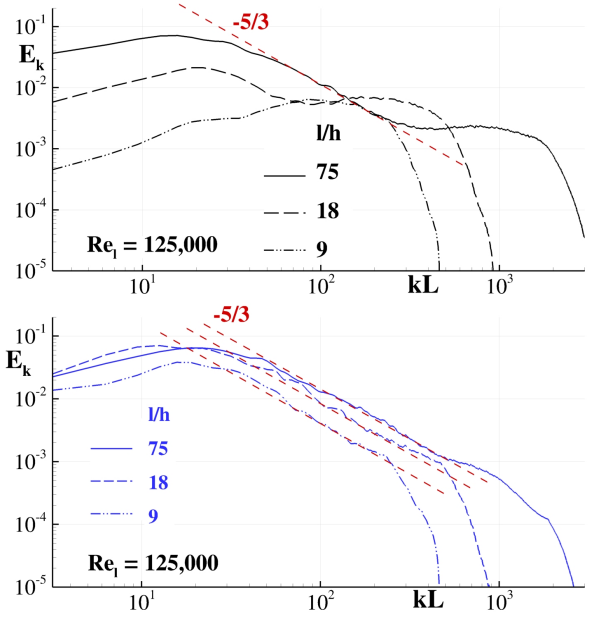

Fig. 2: Two-dimensional freely-decaying turbulence at non-dimensional time $tU/L = 2$ for $\mathrm{Re}_l = 125,000$. Top: energy spectrum from the standard SPH simulation. Bottom: energy spectrum from the LES-SPH simulation.

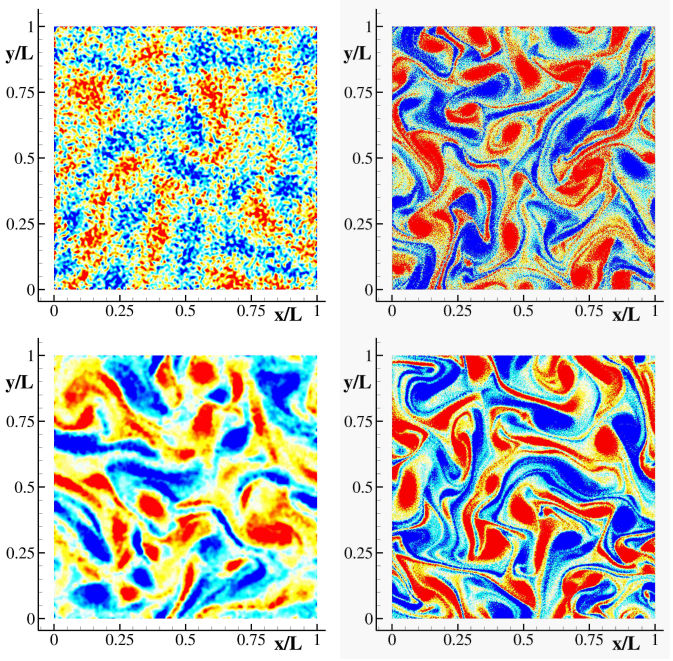

Fig. 3: Two-dimensional freely-decaying turbulence at $\mathrm{Re}_l = 125,000$. Vorticity field at non-dimensional time $tU/L = 2$. Top: standard SPH using spatial resolution l/h equal to 9 (left) and 75(right). Bottom: LES-SPH using spatial resolution l/h equal to 9 (left) and 75 (right).

slope of the spectrum being even opposite to the expected one in most of the range. On the contrary, the finest discretization is able to reproduce the correct energy distribution up to $kL \sim 30$, while for higher frequencies the spectrum attains a non-physical plateau that unveils a dissipation connected with the numerical approximation rather than with physical phenomena. Conversely, when performing LES simulations, the portion of the spectrum related to the inverse cascade (i.e. slope $-5/3$) is correctly captured with all the particle spacings adopted, while for higher frequencies the energy content quickly drops, because of modelling effects. As expected, the amount of resolved energy increases when refining the discretization, as shown by the upward shift of the curves. On the base of the results obtained with the finest resolution it is possible to estimate *a posteriori* the Kolmogorov length scale as:

$$l_D = \left(\frac{\nu^3}{\epsilon}\right)^{1/4}$$

where ϵ is the rate of dissipation of the kinetic energy. From the above expression it results $l_D \simeq 8\times10^{-5}L$ which confirms that with the adopted resolutions the simulation is far from being a DNS.

Figure 3 shows the computed vorticity field at the dimensionless time $tU/L = 2$ by both standard SPH and LES simulations for coarsest and the finest resolutions; in the former case the amount of non-physical noise on the solution is clearly visible in the left plot. As for the the higher

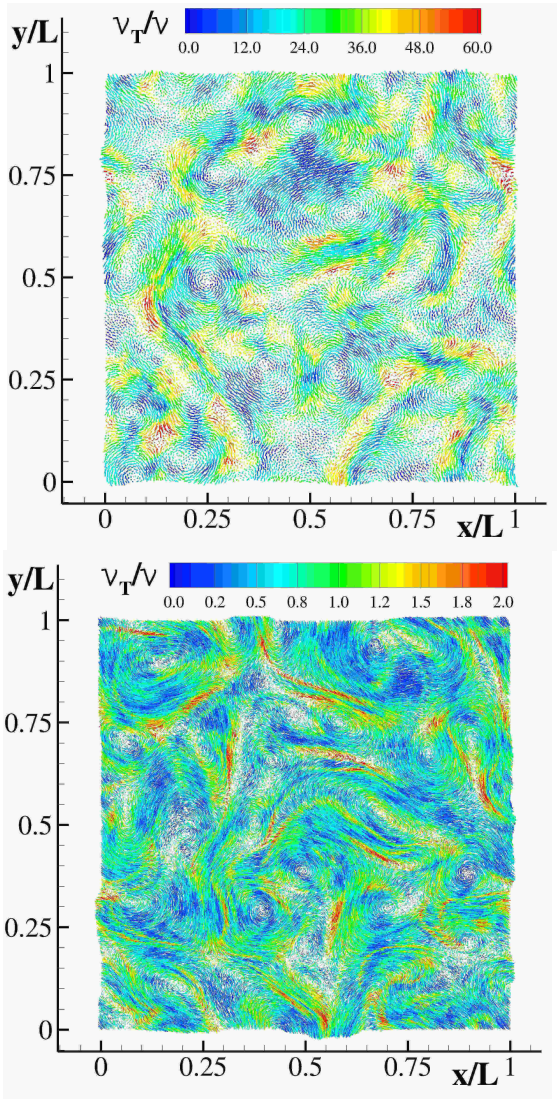

Fig. 4: Two-dimensional freely-decaying turbulence at $\mathrm{Re}_l = 125,000$. Contour plot of the ratio ν_T/ν at non dimensional time $tU/L = 2$, using different spatial resolutions $l/h = 9$ (top) and $l/h = 75$ (bottom).

resolution the vortex structures are better described but the vorticity field is affected by high-frequency noise, which is consistent with the plateau observed in the energy spectrum at high wave numbers. Conversely, the LES-SPH model provides a smoother vorticity field, even at coarse resolution.

The increase of resolved energy with finer discretizations is further confirmed by the values of the eddy viscosity, displayed in figure 4. In fact, for $l/h = 18$ the computed maximum eddy viscosity was 60 times larger than the physical viscosity; for the finest resolution, this ratio drops to about 2.

For a chosen spatial resolution, we observe an increase of about 30% of the computational costs of the LES-SPH models with respect to the DNS simulations. This behaviour is the same for both the Reynolds numbers.

B. Decay of homogeneous turbulence in 3D

As a proof of concept for the proposed filtering in three dimensions, in the present section we report the simulations of homogeneous turbulence for various values of the Reynolds number. The simulations are carried out in a tri-periodic box, namely $0 < x_i < 2\pi L$ with $i = 1, 2, 3$ and $L = 1$, and the initial conditions are generated in the Fourier space as in [39].

In particular, the Fourier components of the velocity are computed as

$$\hat{\boldsymbol{u}}_i(\boldsymbol{\kappa}) = \alpha \boldsymbol{e}_i^1 + \beta \boldsymbol{e}_i^2 \,, \tag{25}$$

where $\boldsymbol{e}_i^1$ and $\boldsymbol{e}_i^2$ are two mutually orthogonal unit vector in the plane orthogonal to the wave vector $\boldsymbol{\kappa}$. The complex coefficients α and β are given by:

$$\alpha = \frac{E(\kappa)}{4\pi\kappa^2} \exp\left(i\theta_1\right) \cos\left(\phi\right) \,, \quad \beta = \frac{E(\kappa)}{4\pi\kappa^2} \exp\left(i\theta_2\right) \sin\left(\phi\right) \,, \tag{26}$$

where θ_1, θ_2 and ϕ are uniformly distributed random numbers on the interval $(0, 2\pi)$ and $\kappa = |\boldsymbol{\kappa}|$. The spectrum $E(\kappa)$ is assumed as

$$E(\kappa) = \frac{q^2}{2A} \frac{\kappa^\varsigma}{\kappa_p^{\varsigma+1}} \exp\left[-\frac{\varsigma}{2}\left(\frac{\kappa}{\kappa_p}\right)^2\right] \,, \tag{27}$$

where $\kappa_p = 9$ is the wave number at which the spectrum is maximum, $\varsigma = 4$, $q^2 = 3$ and A is computed so that the initial turbulence intensity is unitary. The latter, $U = \sqrt{q^2/3}$ is taken as reference velocity. Since the actual computation is in the real space, the velocity vector is computed as:

$$\tilde{\boldsymbol{u}}(\tilde{\boldsymbol{x}}_p, 0) = \Re\big(\mathcal{F}^{-1}[\hat{\boldsymbol{u}}]\big) \tag{28}$$

where $\mathcal{F}^{-1}[\hat{\boldsymbol{u}}]$ is the inverse Fourier transform of $\hat{\boldsymbol{u}}$ and $\Re$ is the real part. As stated in [39], although rather unrealistic as initial conditions, the spectrum evolves toward the expected shape at a later time. The kinematic viscosity is chosen $\nu = 0.001$ and the initial value of the Reynolds number based on the Taylor microscale λ, i.e. :

$$\mathrm{Re}_\lambda = \frac{q^2}{2}\sqrt{\frac{20}{3\,\nu\epsilon}}$$

($\epsilon = -\partial E/\partial t$ being the dissipation rate) is around 1500, whereas it drops to 500 at the final time $tU/L = 5$. The simulations were carried out with three different discretizations, namely 64^3, 128^3 and 256^3 particles initially arranged on a Cartesian lattice. The Kolmogorov scale at the beginning of the simulation is:

$$l_D = \left(\frac{\nu^3}{\epsilon}\right)^{1/4} \simeq 0.02$$

Therefore, for the highest resolution adopted the dissipative scale is close to the particle size. As a consequence, the subgrid model is expected to play an important role for the coarse resolutions while it should be negligible for the highest one. The two coarsest grids were also used to compute the turbulent decay without the proposed LES filtering, in order to highlight its effect. The results are shown in figure 5 for both

simulations, along with the initial spectra. It can be clearly seen that the spectrum evolves towards the expected shape (i.e. with an inertial range with slope $-5/3$) only for the simulations with LES filtering, the direct simulations being too coarse to capture the proper energy cascade.

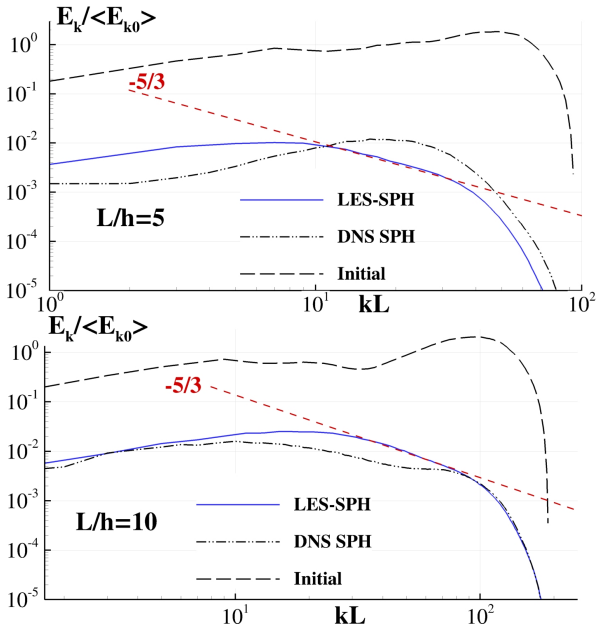

Fig. 5: Three-dimensional homogeneous turbulence decay. Comparison between DNS-SPH and LES-SPH simulations at $tU/L = 5$. Top: particle resolution 64^3. Bottom: particle resolution 128^3. Initial spectra are also shown. The spectra are scaled with the average initial kinetic energy $< E_{k0} >$.

The comparison of the simulations for the three particle resolutions is shown in figure 6, where it can be clearly seen that, as expected, the amount of resolved kinetic energy increases with the resolution, because the reduced particle spacing is driving the simulation toward a resolved direct simulation.

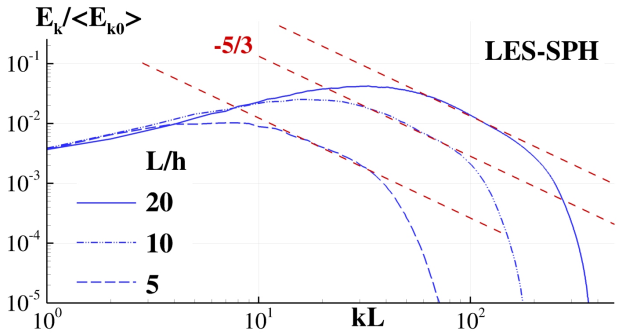

Fig. 6: Three-dimensional homogeneous turbulence decay. Comparison among different resolutions at $tU/L = 5$. The spectra are scaled with the average initial kinetic energy $< E_{k0} >$.

Similarly to the 2D case, the increase of resolved energy when refining the resolution can be observed by comparing the eddy viscosity fields, displayed in figure 7. For $L/h = 20$ the computed maximum eddy viscosity is only a fraction of the physical viscosity since the adopted resolution is close to the Kolmogorov scale at this Re_λ and, therefore, the simulation is close a DNS; conversely, for $L/h = 20$ the modelled energy is larger and is comparable to the resolved one as the observed ratio ν_T/ν is close to 1.

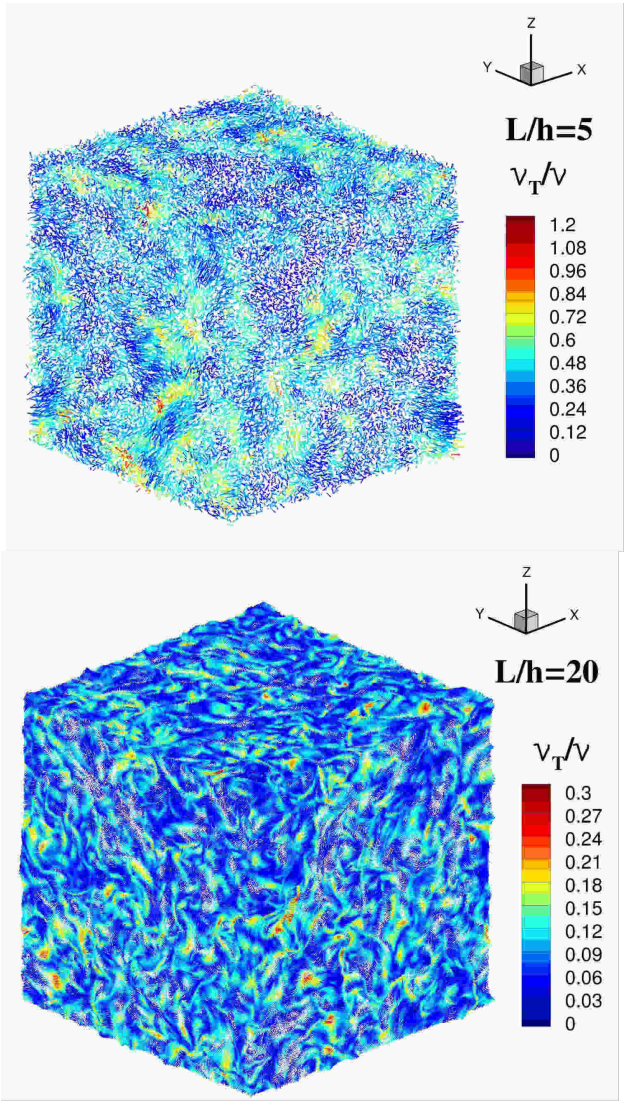

Fig. 7: Three-dimensional homogeneous turbulence decay at $tU/L = 5$ ($\mathrm{Re}_\lambda = 500$). Contour plot of the ratio ν_T/ν using spatial resolutions $L/h = 5$ (top) and $L/h = 20$ (bottom).

VI. Conclusion and Perspectives

In the present paper, a general LES-SPH model is defined. First, Large Eddy Simulation is reformulated in a Lagrangian context by filtering all the variables in both time and space; this procedure allows maintaining the Lagrangian structure of the Navier–Stokes equations in term of material derivatives computed on particles that move with the filtered velocity.

The Lagrangian formulation of LES is then used to re–interpret the SPH approximation of differential operators as a specific model based on the decomposition of the LES filter into a spatial and time filter. The derived equations represent a general LES-SPH scheme and contain terms that in part come from LES filtering and in part derive from SPH kernels. The last ones lead to additional terms (with respect to LES filtering) that contain fluctuations in space, requiring adequate modeling. Finally, a closure of the LES-SPH scheme is proposed; the scheme is recast in fashion similar to the diffusive SPH scheme of Molteni & Colagrossi [2] in which diffusive terms are dependent on the local features of the velocity field- Some numerical simulations are reported for free decay of two– and three–dimensional homogeneous and isotropic turbulence. The obtained results prove that the expected characteristics of the flow evolution are well captured by SPH simulations with relatively coarse particle discretization, if the correct LES modeling is included.

It is to be underlined that no rigorous calibration of the coefficients that appear in the model has been performed yet, because the main goal of the paper was to outline a correct LES filtering procedure in the SPH framework.

ACKNOWLEDGEMENTS

Work partially supported by the Flagship Project RITMARE - Italian Research for the Sea - coordinated by Italian National Research Council and funded by Italian Ministry of Education, University and Research within Nat. Res. Program 2015-2016. The SPH simulations performed in the present research have been obtained using the SPH-flow solver, software developed within a collaborative consortium composed of Ecole Centrale de Nantes, NEXTFLOW Software company and CNR-INSEAN.

REFERENCES

[1] A. Di Mascio, M. Antuono, A. Colagrossi, and S. Marrone, "Smoothed particle hydrodynamics method from a large eddy simulation perspective," *Physics of Fluids*, vol. 29, no. 3, p. 035102, 2017.

[2] D. Molteni and A. Colagrossi, "A simple procedure to improve the pressure evaluation in hydrodynamic context using the SPH," *Computer Physics Communications*, vol. 180, pp. 861–872, 2009.

[3] D. Wilcox, "Turbulence modeling for CFD," *DCW industries La Canada*, vol. 2, 1992.

[4] D. Violeau and R. Issa, "Numerical modelling of complex turbulent free surface flows with the SPH Lagrangian method: an overview," *Int. J. Num. Meth. Fluids*, vol. 53(2), pp. 277–304, 2006.

[5] D. De Padova, M. Mossa, and S. Sibilla, "SPH numerical investigation of the velocity field and vorticity generation within a hydrofoil-induced spilling breaker," *Environmental Fluid Mechanics*, vol. 16, no. 1, pp. 267–287, 2016.

[6] A. Leroy, D. Violeau, M. Ferrand, and C. Kassiotis, "Unified semi-analytical wall boundary conditions for 2-D incompressible SPH," *J. Comput. Phys.*, vol. 261, pp. 106–129, 2014.

[7] M. Lesieur and O. Métais, "New trends in large-eddy simulations of turbulence", *Annual Review of Fluid Mechanics*," *Annual Review of Fluid Mechanics*, vol. 28, pp. 45–82, 1996.

[8] U. Piomelli, "Large-eddy simulation: achievements and challenges", *Progress in Aerospace Sciences*," *Progress in Aerospace Sciences*, vol. 35, no. 4, pp. 335–362, 1999.

[9] C. Meneveau and J. Katz, "Scale-invariance and turbulence models for large-eddy simulation," *Annual Review of Fluid Mechanics*, vol. 32, no. 1, pp. 1–32, 2000.

[10] "Wall-layer models for large-eddy simulations," *Annual review of fluid mechanics*, vol. 34, no. 1, pp. 349–374, 2002.

[11] P. R. Spalart, "Trends in turbulence treatments," *American Institute of Aeronautics and Astronautics*, 2000.

[12] H. Gotoh, T. Shibahara, and T. Sakai, "Sub-particle-scale turbulence model for the MPS method - Lagrangian flow model for hydraulic engineering," *Advanced Methods for Computational Fluid Dynamics*, vol. 9, no. 4, pp. 339–347, 2001.

[13] D. Violeau, S. Piccon, and J. Chabard, "Two attempts of turbulence modelling in Smoothed Particle Hydrodynamics," vol. 4. Proceedings of the 8th International Symposium on Flow Modeling and Turbulence Measurements, 2001, p. 6.

[14] E. Lo and S. D. Shao, "Simulation of near-shore solitary wave mechanics by an incompressible SPH method," *Applied Ocean Research*, vol. 24, no. 5, pp. 275–286, 2002.

[15] R. Dalrymple and B. Rogers, "Numerical modeling of water waves with the SPH method," *Coastal Engineering*, vol. 53 (2-3), pp. 141–147, 2006.

[16] J. Monaghan, "Simulating Free Surface Flows with SPH," *Journal of Computational Physics*, vol. 110, no. 2, pp. 39–406, 1994.

[17] S. Marrone, A. Colagrossi, A. Di Mascio, and D. Le Touzé, "Prediction of energy losses in water impacts using incompressible and weakly compressible models," *Journal of Fluids and Structures*, vol. 54, pp. 802–822, 2015.

[18] M. Germano, U. Piomelli, P. Moin, and W. Cabot, "A dynamic subgrid-scale eddy viscosity model," *Physics of Fluids A: Fluid Dynamics*, vol. 3, no. 7, pp. 1760–1765, 1991.

[19] A. Colagrossi, M. Antuono, and D. Le Touzé, "Theoretical considerations on the free-surface role in the Smoothed-particle-hydrodynamics model," *Physical Review E*, vol. 79, no. 5, p. 056701, 2009.

[20] A. Colagrossi, M. Antuono, A. Souto-Iglesias, and D. Le Touzé, "Theoretical analysis and numerical verification of the consistency of viscous smoothed-particle-hydrodynamics formulations in simulating free-surface flows," *Physical Review E*, vol. 84, p. 026705, 2011.

[21] P. Moin, K. Squires, W. Cabot, and S. Lee, "A dynamic subgrid-scale model for compressible turbulence and scalar transport," *Physics of Fluids A*, vol. 3, no. 11, pp. 2746–2757, 1991.

[22] A. Yoshizawa, "Statistical theory for compressible turbulent shear flows, with the application to subgrid modeling," *Physics of Fluids*, vol. 29, p. 2152, 1986.

[23] G. Blaisdell, N. Mansour, and W. Reynolds, "Compressibility effects on the growth and structure of homogeneous turbulent shear flow," *Journal of Fluid Mechanics*, vol. 256, pp. 443–485, 1993.

[24] T. Passot and A. Pouquet, "Numerical simulation of compressible homogeneous flows in the turbulent regime," *Journal of Fluid Mechanics*, vol. 181, pp. 441–466, 1987.

[25] J. Suh, S. Frankel, L. Mongeau, and M. Plesniak, "Compressible large eddy simulations of wall-bounded turbulent flows using a semi-implicit numerical scheme for low Mach number aeroacoustics," *Journal of Computational Physics*, vol. 215, no. 2, pp. 526–551, 2006.

[26] J. P. Morris, P. J. Fox, and Y. Zhu, "Modeling Low Reynolds Number Incompressible Flows Using SPH," *Journal of Computational Physics*, vol. 136, pp. 214–226, 1997.

[27] J. J. Monaghan, "Smoothed particle hydrodynamics," *Reports on Progress in Physics*, vol. 68, pp. 1703–1759, 2005.

[28] J. Monaghan and R. A. Gingold, "Shock Simulation by the particle method SPH," *Journal of Computational Physics*, vol. 52, no. 2, pp. 374–389, 1983.

[29] T. Belytschko, Y. Krongauz, J. Dolbow, and C. Gerlach, "On the completeness of meshfree particle methods," *Int. J. Numer. Methods Engineering*, vol. 43, no. 5, pp. 785–819, Nov. 1998.

[30] M. Antuono, A. Colagrossi, S. Marrone, and D. Molteni, "Free-surface flows solved by means of SPH schemes with numerical diffusive terms," *Computer Physics Communications*, vol. 181, no. 3, pp. 532–549, 2010.

[31] S. Marrone, M. Antuono, A. Colagrossi, G. Colicchio, D. Le Touzé, and G. Graziani, "Delta-SPH model for simulating violent impact flows," *Computer Methods in Applied Mechanics and Engineering*, vol. 200, no. 13-16, pp. 1526–1542, 2011.

[32] M. Antuono, A. Colagrossi, and S. Marrone, "Numerical diffusive terms in weakly-compressible SPH schemes," *Computer Physics Communications*, vol. 183, no. 12, pp. 2570–2580, 2012.

[33] A. Colagrossi, A. Souto-Iglesias, M. Antuono, and S. Marrone, "Smoothed-particle-hydrodynamics modeling of dissipation mechanisms in gravity waves," *Physical Review E*, vol. 87, p. 023302, 2013.
[34] A. Colagrossi, B. Bouscasse, M. Antuono, and S. Marrone, "Particle packing algorithm for SPH schemes," *Computer Physics Communications*, vol. 183, no. 2, pp. 1641–1683, 2012.
[35] M. Antuono, B. Bouscasse, A. Colagrossi, and S. Marrone, "A measure of spatial disorder in particle methods," *Computer Physics Communications*, vol. 185, no. 10, pp. 2609–2621, 2014.
[36] Y. Shi, X. Zhu, M. Ellero, and N. Adams, "Analysis of interpolation schemes for the accurate estimation of energy spectrum in Lagrangian methods," *Computers & Fluids*, vol. 82, pp. 122–131, 2013.
[37] P. Tabeling, "Two-dimensional turbulence: a physicist approach," *Physics Reports*, vol. 362, no. 1, pp. 1–62, 2002.
[38] J. W. Swegle, D. L. Hicks, and S. W. Attaway, "Smoothed Particle Hydrodynamics Stability Analysis," *Journal of Computational Physics*, vol. 116, pp. 123–134, 1995.
[39] N. Mansour and A. Wray, "Decay of isotropic turbulence at low Reynolds number," *Physics of Fluids*, vol. 6, no. 2, pp. 808–814, 1994.